AMINO ACIDS IN THE FIRST TRANSMEMBRANE DOMAIN AFFECTING FUNCTION OF THE EXTRACELLULAR DOMAIN OF TRUNCATED A4B2 CHIMERAS OF THE NICOTINIC ACETYLCHOLINE RECEPTOR

An Undergraduate Research Scholars Thesis

by

ADRI MICHELLE GALVAN

Submitted to Honors and Undergraduate Research
Texas A&M University
in partial fulfillment of the requirements for the designation as an

UNDERGRADUATE RESEARCH SCHOLAR

Approved by
Research Advisor: Dr. Gregg Wells

May 2015

Major: Molecular and Cell Biology

TABLE OF CONTENTS

ABSTRACT

Amino Acids in the First Transmembrane Domain Affecting Function of the Extracellular Domain of Truncated α4β2 Chimeras of the Nicotinic Acetylcholine Receptor. (May 2015)

Adri Michelle Galvan
Department of Biology
Texas A&M University

Research Advisor: Dr. Gregg Wells
Department of Molecular and Cellular Medicine
Texas A&M Health Science Center

Important neurological and psychiatric diseases, including Alzheimer disease, nicotine addiction, and schizophrenia, are influenced by nicotinic acetylcholine receptors (nAChRs). Understanding the structure and function of nAChRs will provide a foundation for developing drug therapies for these diseases. nAChRs are members of the Cys-loop receptor superfamily. Each nAChR contains five subunits with each subunit containing four transmembrane domains. Once the ligand binds to the extracellular domain (ECD), the section of the nAChR that is exposed to the external environment, the protein undergoes a conformation change and an ion flux occurs allowing signal transmission. The first transmembrane domain (M1) is specifically critical for the function of the neurotransmitter-binding ECD in nAChRs. The features of M1 that are essential for ECD function, however, are not fully known. M1 sequences from ionotropic serotonin (5HT3A) and from α4, β2, and α7 nAChR subunits are similar but behave differently in ECD α4β2 nAChRs. The sequence differences provide the opportunity to discover amino acids from M1 that promote or inhibit ECD function. Through site-directed mutagenesis and expression of chimeric M1 domains with extracellular α4 and β2 subunits in *Xenopus* oocytes, we determined amino acids in native M1 controlling expression of ECD α4β2 nAChRs and

amino acids from the 5HT3A M1 inhibiting that expression. Generating a feasible ECD will provide insight into the essential properties allowing proper ligand binding, conformational changes, and in result the ion cascade triggering the receptor's function. The truncated designs of full length receptors will contribute to understanding how nAChR subunits fold and assemble and how their transmembrane domains affect structure and function. The results will aid in identifying the importance of M1 in ECD function and guide the development of ECD Cys-loop receptors as water-soluble structural models of the full length receptors. Water-soluble models are a key step in advancing our understanding of nAChRs due to the difficulty of producing high resolution structural models of full-length nAChR through crystallography. With the advantageous physical properties of water-soluble protein, the shortcomings of crystallography with the full-length nAChRs would be overcome, allowing for further understanding of nAChR assembly, function, and future drug design.

ACKNOWLEDGEMENTS

I would like to thank Dr. Wells and Alexi Person for their contributions to this study and their continual support and mentorship. I would also like to thank Alexi for performing the necessary *Xenopus laevis* surgeries and oocyte injections.

NOMENCLATURE

nAChR	Nicotinic Acetylcholine Receptor
M1-M4	Transmembrane Domains 1-4
5HT3A	Serotonin Receptor
ECD	Extracellular Domain
GluCl	Glutamate Receptor
AChR	Acetylcholine Receptor
NMR	Nuclear Magnetic Resonance
AChBP	Acetylcholine Binding Protein
ELIC	*Erwinia chrysanthemi*
GLIC	*Gloeobacter violaceus*
DPM	Disintegrations per Minute

CHAPTER I

INTRODUCTION

Nicotinic acetylcholine receptors (nAChRs) are cationic Cys-loop ligand-gated ion channel receptors characterized by their five subunit composition with each containing four transmembrane domains (M1-M4).[1] The cation conducting receptors of the Cys-loop ligand-gated ion channel superfamily are nAChR and serotonin (5HT3A).[1] Sixteen different subunits makeup the nAChR subunit family with α4, α7 and β2 being some of the most common types in humans.[2] Essential elements of the nAChRs include an amino terminus extracellular domain (ECD) containing a Cys-loop, three conserved transmembrane domains and a fourth more inconsistent transmembrane domain, an intracellular cytoplasmic loop between the third and fourth transmembrane domain, and a carboxyl terminus.[1]

The entire ligand-gated ion channel superfamily, including GABA A, glycine, serotonin (5HT3A), some glutamate (GluCl), and acetylcholine receptors (AChR), holds vast pharmacological potential with their neurotransmitter-activated receptors impacting the central and peripheral nervous systems.[3] nAChRs are known specifically for playing a role in neurodegenerative diseases such as Alzheimer disease and schizophrenia. The function of nAChRs decrease with the progression of neurodegenerative disease, therefore understanding the receptor's structure and the ligand binding domain is important for developing therapies. Pursuit of structural understanding of the receptor has been underway for decades, although only relatively recently have crystallography and NMR techniques contributed with studies of model structures. Full-length nAChR proteins cannot currently be produced at high enough

concentrations for high resolution structural studies.[2] Attaining water-soluble models of the nAChRs would overcome limitations, such as hydrophobicity and instability, associated with crystallizing full-length transmembrane proteins. In result, experimental procedures to generate water-soluble protein at great enough levels for crystallization and consequently drug therapy studies have been the focus of many studies.

The quest for the production of potential drug designs for nAChRs began with the crystallization of a homologous receptor, the acetylcholine binding protein (AChBP).[4] With 20-24% of the AChBP's ECD being identical to the ECD of nAChRs, this structural data allowed for more insight into the nAChR construct.[4] Crystallography of a bacterial ligand gated ion channel from *Erwinia chrysanthemi* (ELIC), now referred to as *Dickeya dadantii*, and *Gloeobacter violaceus* (GLIC) also allowed for a comparable analysis of the crystallized structure to nAChRs.[5, 6] The next breakthrough for our understanding of nAChRs was the electron microscopy image generated from the muscle nAChR of *Torpedo marmorata*.[7] Then in 2007, the nAChR subunit α1 ECD was crystallized while bound with α-bungarotoxin, an antagonistic neurotoxin.[8] This study elucidated the role of essential components and residues for the binding of a ligand to the nAChR.

Other studies have recently contributed to our overall comprehension of the ligand binding mechanism. For example, glycosylation was found to be unessential for proper binding abilities.[9] This was a significant discovery as it is easier to crystallize deglycosylated proteins.[10] nAChR studies have also concluded that replacing the hydrophobic Cys-loop region of the receptor with a similar hydrophilic section allows for better expression, but the proper subunit

association and receptor binding abilities have yet to be achieved.[9] Replacing the Cys-loop of the nAChR with the Cys-loop of the AChBP allowed increased solubility and expression as well.[11] However, the proper subunit association critical for binding abilities was impeded and the protein had low affinities for ligands.[11] Concatamerized and truncated proteins have been created in hopes of producing proteins that have high expression yields, are soluble for crystallization purposes and retain the functional ability of the receptor with a high binding affinity for ligands.[11, 12] Experiments have also been conducted to analyze the role of linkers in creating covalently bound subunits leading to operative receptors.[9] While all of these advancements have led to a deeper understanding of nAChRs, low resolution structures and an inability to form pentameric structures in sufficient yield for crystallization have been continual obstacles.

As we strive to create feasible water soluble receptors in order to produce crystallizable models, eliminating flexible regions of the subunits such as the M3M4 intracellular loop could be a possible way to create these models.[13] Interestingly, the M3M4 intracellular loops of ligand-gated ion channel bacterial homologs were found to be much smaller than the large intracellular loops in eukaryotic receptors.[5, 6] It was then discovered that in 5HT3A receptors the native M3M4 loop was not essential for proper subunit assembly or receptor function.[14] This same concept was applied to a nAChR and GluCl-β chimera and the truncated M3M4 loop allowed function unlike the results seen with a pure nAChR.[14] However, when the entire loop was removed the receptor no longer functioned.[14] It was concluded that at least a heptapeptide, as present in ELIC, was necessary for a feasible receptor.[14] The M3M4 loop is a significant factor

to consider when constructing a water soluble model due to the fact that the loop is believed to play a role in proper receptor assembly and the desensitization of the receptor when activated.[14]

Recent x-ray crystallography of 5HT3A, ionotropic glutamate receptor α (GluCl), and GABAA have also contributed to our understanding of the Cys-loop receptor superfamily.[15-17] However, only homomers were crystallized still leaving questions on the assembly and structure of heteromers often seen in nAChRs. The GluCl is of specific interest due to the similar folding of the transmembrane helices when compared to nAChRs.[18] The amino acid sequence and protein structure of GluCl and nAChR are clearly related, but a discrepancy arises as the M2 and M3 show significant variation.[18] GluCl also has a serine residue believed to be critical in ligand binding and activation while nAChRs lack this residue.[18] These inexplicable differences between nAChRs and GluCl are important to be aware of when studying the structures of the receptors and the mechanisms of function. The crystallography of 5HT3A may hold even more importance in our pursuit to grasp the role of structure in the nAChR function. 5HT3A receptors are very similar to nAChRs and their comparability has been exploited as researchers have sought to create chimeric pentamer proteins with functional binding sites.[19] A nAChR α7-5HT3A chimera with a functional binding site was successfully produced while a homopentamer composed of α7 subunits lacked this property.[19] This study has led to many investigations into the differences between the homologs. Our study strives to contribute to this understanding as we search for key residues distinguishing the function of the α7 and 5HT3A receptors.

As research continues to develop our understanding of Cys-loop receptors through crystallized structures, scientists have sought to determine how else we can manipulate the production of

nAChR through various model systems for heterologous expression of proteins. *Pichia pastoris*, a yeast system, *Spodoptera frugiperda*, an insect system, and *Xenopus laevis*, a frog system, have all been used for research. However, a limitation arose in the yeast models as expressing receptors with more than two subunits were not feasible.[9] Our model system, *Xenopus laevis*, is particularly suited for this project as past research has shown that functioning heterologous receptors such as α4β2 can be produced.[20] Having the ability to produce viable α4β2 receptors is an important property of *Xenopus* as this receptor is the most common type within the brain.[21]

The significant advancements made throughout the Cys-loop receptor family has allowed us to gain much more insight into the structural basis of the function of nAChR receptors. We know that the α4 and β2 subunits act together to form the binding region for the ligand.[22] The α4 subunit comprises most of the binding face and the Cys-loop is known to be essential for proper ligand association as well.[22] However, our understanding of orthosteric ligand binding, where binding occurs at the active site of the protein, and its impact on the nAChRs receptors are still too limited for drug design.[2] Our research studies the feasibility of creating high fidelity models of the ECD of nAChRs. Water soluble designs offer the possibility of higher resolution structures than is possible with full-length transmembrane domain constructs consequently allowing for more defined crystallography models.[13] These truncated designs of full length receptors will contribute to understanding how nAChR subunits fold and assemble and how their transmembrane domains affect structure and function.

The first transmembrane domain (M1) of nAChR has been found to be specifically critical for the function of the neurotransmitter-binding extracellular domain.[23] While M1 is fundamental in

heterodimer formation of nAChRs, the features of M1 that are essential for extracellular domain function have not been fully exploited.[24] M1 sequences from ionotropic serotonin (5HT3A) and from α4, β2, and α7 nAChR subunits are similar but behave differently in ECD α4β2 nAChRs (Fig. 1). The structural and sequence similarity between the two receptor families allows for structural comparison and analysis.

```
m5HT3A        PLFYAVSLLLPSIFLMVVDIVGFCLPP
Chα7M1        -LYYGLNLLIPCVLISALALLVFLLP-
Humα4M1       PLFYTINLIIPCLLISCLTVLVFYL--
Humβ2M1       PLFYTINLIIPCVLITSLAILVFYL--
               *:* :.*::*.:::  : :: * *
```

Figure 1. Protein comparison of the M1 domain from human α4, human β2, chicken α7, and mouse 5HT3A.

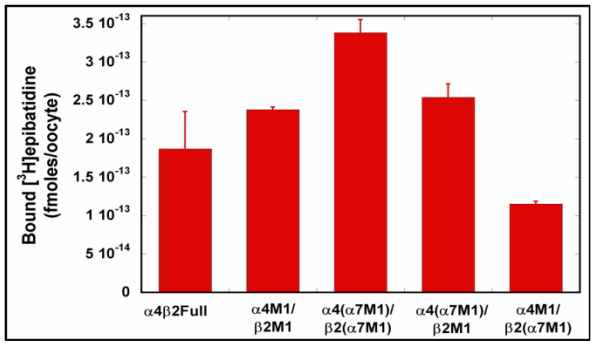

Figure 2. [^{3}H]epibatidine binding graph of α4α7M1 and β2α7M1 nAChR chimeras. Concludes that α4β2 nAChRs M1 can be replaced by α7M1 and retain the [^{3}H]epibatidine high affinity.[23]

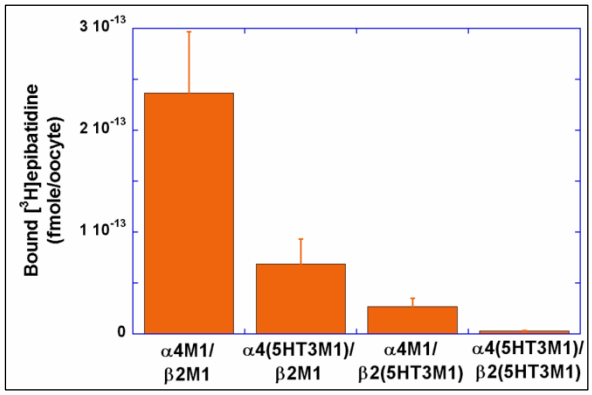

Figure 3. [^{3}H]epibatidine graph of α4M/β2M1, α4(5HT3M1)/β2M, α4M1/β2(5HT3M1), and α4(5HT3M1)/β2(5HT3M1). Concludes that α4β2 nAChRs M1 cannot be replaced by 5HT3M1 and retain high [^{3}H]epibatidine affinity.[23]

Experiments have shown that M1 from α4 and β2 nAChR subunits can be replaced with M1 from the α7 subunit while maintaining the ligand binding function of the extracellular domain (Fig. 2).[23] In contrast, replacing native M1 with M1 from the 5HT3A Cys-loop subunit abolishes ligand binding function (Fig. 3).[23] Other particular amino acids, such as cysteines and prolines, have been found to be indispensable for the function of the nAChR extracellular domain.[25] Previous studies have also shown that the first half of M1 is critical for extracellular domain function.[23] Our experiment will use this formative knowledge to guide our study of the nAChR M1 and its role in the receptor's function.

Through this research, we seek to determine amino acids in native M1 controlling expression of the ECD of α4β2 nAChR and amino acids from the 5HT3A M1 inhibiting that expression. Our objectives are to identify the importance of M1 and guide the development of ECD Cys-loop receptors as water-soluble structural models of the full length transmembrane receptors. With these intentions, we seek to advance toward our goal of understanding the structure and function of nAChR providing a foundation for developing drug therapies for neurological and psychiatric diseases for all Cys-loop receptors.

CHAPTER II

METHODS

Design of α7-5HT3A M1 Chimeras

Beginning with protein comparisons using EMBOSS Water Pairwise Sequence Alignment based on the BLOSUM 62 matrix, the amino acids of the M1 regions of chicken (ch) nAChR α7 and mouse (m) 5HT3A were ranked according to their degree of similarity (Fig. 4). The colored residues represent most conserved to least conserved denoted by yellow to green to blue and finally red.

```
Chα7M1       -LYYGLNLLIPCVLISALALLVFLLP-
m5HT3A       PLFYAVSLLLPSIFLMVVDIVGFCLPP
              *:*.:.**:*.::: .: :: * **
```

Figure 4. An amino acid comparison of chα7 and m5HT3A M1.

The amino acid disparities were then grouped into tentative parts ranging from a predicted preservation of ECD function to a predicted loss of function when converted from α7 to 5HT3A residues. Ten distinct constructs were outlined using OMIGA with varying amounts of residue changes (Fig. 5). The addition of yellow to green to blue to red residues represents the hypothesized progression of deleterious effects on the receptor. The constructs were arranged in two ways: collective mutations, where the effects of the rising number of mutations can be seen, and independent mutations, where the effects of the different mutation types are seen individually.

Control α4M1α7	LYYGLNLLIPCVLISALALLVFLLP	Control β2M1α7	LYYGLNLLIPCVLISALALLVFLLP
Part1α4M1α7-5HT3A	LFYGVNLLLPCILLSAVAIVVFLLP	Part1β2M1α7-5HT3A	LFYGVNLLLPCILLSAVAIVVFLLP
Part1bα4M1α7-5HT3A	LFYGVNLLLPCILISALALLVFLLP	Part1bβ2M1α7-5HT3A	LFYGVNLLLPCILISALALLVFLLP
Part1cα4M1α7-5HT3A	LYYGLNLLIPCVLLSAVAIVVFLLP	Part1cβ2M1α7-5HT3A	LYYGLNLLIPCVLLSAVAIVVFLLP
Part2α4M1α7-5HT3A	LFYGVNLLLPCIFLMVVAIVGFLLP	Part2β2M1α7-5HT3A	LFYGVNLLLPCIFLMVVAIVGFLLP

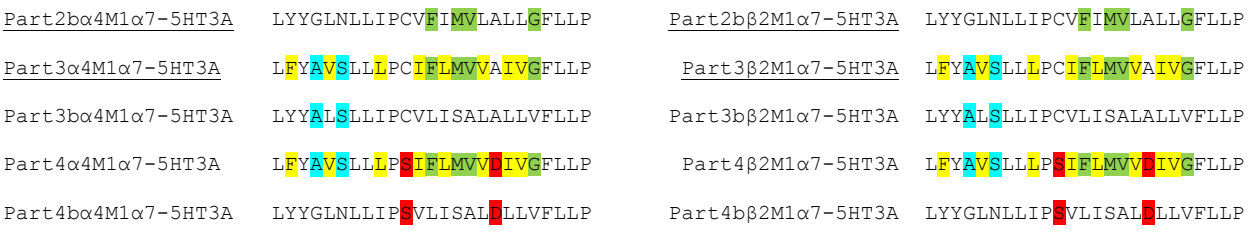

Figure 5. Ten chα7-m5HT3A chimeric constructs designed to cause progressive loss of ECD function.

Construction of nAChR Chimeras

Using DNA synthesis services, DNA 2.0 and IDT, the site-directed mutations from chα7 to m5HT3A amino acids established through the sequence studies were synthesized. The DNA then underwent a bacterial transformation using One Shot® OmniMAX™ 2 T1 Chemically Competent E.coli (Invitrogen) cells. After obtaining a sufficient amount of DNA in bacteria, a QIAfilter® Plasmid Midi Prep Kit (Qiagen) was performed to purify the DNA. To ensure the desired designs were produced double digestions were performed. The sequence of the chα7-m5HT3A M1 chimera within the DNA 2.0/IDT vector was then cleaved using the restriction enzymes EagI-HF and MluI and BstXI and MluI (New England BioLabs) for the α4 and β2 constructs, respectively. The double digest gels from the previous step were consequently isolated using Zymoclean™ Gel DNA Recovery Kit (Zymo Research). α4β2 α7-5HT3A M1 chimeras were then ligated with the ECD of human α4 and human β2 subunits in a pSP64 Poly(A) vector (Promega) using T4 DNA Ligase (New England BioLabs). A bacterial transformation was performed with the newly made chimera and the Zyppy™ Plasmid Miniprep Kit (Zymo Research) was used to purify the DNA. Double digestions were then done to ensure the proper sequences were present. After confirming the presence of the desired gene product, QIAfilter® Plasmid Midi Prep Kit (Qiagen) was used to purify a greater amount of DNA. Lone Star Labs DNA sequencing was then used to verify that the proper sequences were present. The

vectors were then linearized using restriction enzymes AseI and PvuII to cut the α4 and β2 constructs, respectively, and Ambion mMessage mMachine® SP6 Kit was used to produce RNA from the linearized DNA. Gel electrophoresis was used throughout this process to confirm the presence of appropriate band lengths and consequently the presence of the correct DNA and RNA.

Xenopus Oocyte Injections and Protein Production

Oocytes were surgically extracted from *Xenopus laevis* and were prepared using collagenase type I (Invitrogen) in order to remove the vascular layer incasing the oocyte. A 40 nl aliquot containing 20 ng of the nAChR chimera RNA was injected into the cytoplasm of the vegetal pole of each oocyte. This procedure was replicated for each designed subunit construct. The oocytes were then incubated at 18°C for 3 days in 50% Leibovitz's L-15 medium (Invitrogen) in 10 mM HEPES (Sigma), pH 7.5, containing 10 units/ml penicillin (Invitrogen), 10 µg/ml streptomycin (Invitrogen), and 43 µg/ml gentamicin (Invitrogen). Following this step, the desired protein product was isolated by homogenizing 25-50 oocytes by hand in an ice-cold buffer (Buffer A: in mM: 50 sodium phosphate, 50 NaCl, 5 EDTA, 5 EGTA, 5 benzamidine, 15 iodoacetamide, pH 7.5), centrifuging the solution for 30 minutes at 14,500 x g at 4°C, and consequently solubilizing the pellet in a buffer (Buffer B: Buffer A with 2% w/v Triton X-100) with gentle agitation for 2 hours at 4°C. Centrifugation was then repeated (30 minutes, 14,500 x g, 4°C) and the detergent extract containing the anticipated protein product was consequently removed. The isolated supernatant was then divided for use in immunoblotting and ligand binding assays.

[^{3}H]Epibatidine Testing

Ligand binding assays with [^{3}H]epibatidine were conducted to identify the ligand dissociation constant and the yield of the resulting ECD receptors. The ligand dissociation constant measures the fidelity of the ECD structure to the structure of the full length receptor. The yield of ECD receptors compared to the yield of the full length receptor measures how efficiently the truncated subunits were assembled. Immulon 4 HBX plastic microwells (Thermo Labsystems) for solid phase binding assays were coated with the primary antibody which was diluted in 10 mM CAPSO to a concentration of 4µg/ml of CAPSO and incubated for 3 days. The wells were subsequently washed with NaN_3-PBS. After the wash, the wells were blocked with 3% bovine serum albumin, fraction V (EM Science), in PB +S (in mM: 137 NaCl, 2.7 KCl, 1.4 KH_2PO_4 10 Na_2HPO_4), incubated for 2 hours and washed with wash buffer. A volume of detergent extract from 0.1 to 0.5 injected oocytes was added to the primary antibody-coated microwells. The microwells were incubated overnight at 4°C for proper binding to occur and then washed with ice cold buffer B. 100 µl of (±)-[^{3}H]epibatidine (PerkinElmer Life Sciences; specific activity: 55.8 Ci/mmol) in ice-cold buffer B was then added to each microwell and incubated overnight at 4°C for the purpose of measuring the [^{3}H]epibatidine binding. The microwells were washed again with ice-cold buffer B and stripped with a solution of 5% SDS and 25 mM dithiothreitol in buffer B. A liquid scintillation counter was used to measure the amount of [^{3}H]epibatidine bound for each sample. Data was recorded as the average of duplicate and triplicate measurements.

Immunoblotting Analysis

The presence of the protein product was determined through immunoblot analysis using the mAb 142 and mAb 236 epitope tags for the α4 and β2 chimeras, respectively. Beginning with a 5

minute 65°C denaturation period with 1% SDS and 15 mM dithiothreitol, the samples were then separated by SDS-PAGE on a 12.5% acrylamide gel. Using Bio-Rad Precision Plus- Dual Color (20 µl) for visualization purposes, the gel was run at 15 milliamps for 65 minutes and subsequently 30 milliamps for 90 minutes. The Immun-Blot™ polyvinylidene difluoride (PVDF) membrane (BioRad) was wetted with 100% methanol and then run at 30V for 30 minutes using a GENIE® electrophoretic transfer device (Idea Scientific) in order for protein transfer to occur. After completion of the run, the membrane was re-wetted with methanol to minimize movement of proteins on the membrane. Overnight, the membrane was then blocked at 4°C with blocking buffer (5% powdered milk in PBS buffer and 0.05% Tween®20. The primary antibody, Monoclonal Anti-Nicotinic Acetylcholine Receptor, α4 subunit, Clone mAb142 (Sigma) was diluted 1:10,000 in blocking buffer and incubated with the membrane overnight at 4°C while continuously rocked. Wash buffer (PBS and 0.05% Tween) washed the membrane three times for one hour per wash. The secondary antibody, ImmunoPure® Goat Anti-Rat IgG, (H+L), Peroxidase Conjugated (Pierce), was diluted 1:5000 in blocking buffer and incubated with the membrane overnight at 4°C. Again, the washing procedures were repeated. The SuperSignal West Dura Extended Duration Substrate (Pierce) was used in accordance with the standard protocol so as to visualize the protein products on BioMax ML film (Eastman Kodak Co.).

The gel was then stripped using Restore Western Blot Stripping Buffer (Thermo Scientific). The blot was covered in the stripping buffer and incubated for 15 minutes at 37ºC. After, the blot was washed three times at 30 minutes each with wash buffer. The western blot procedure outlined above was repeated beginning with the blocking buffer. The β2 antibody, mAb236, was

diluted to 1:12,000 in blocking buffer and then the secondary antibody ImmunoPure® Goat Anti-Rat IgG, (H+L), Peroxidase Conjugated (Pierce), was diluted 1:5000 in blocking buffer.

CHAPTER III

RESULTS

Ligand Binding Assay

The binding abilities of the produced proteins were tested using an [^{3}H]epibatidine binding assay. A liquid scintillation counter determined the amount of [^{3}H]epibatidine bound to the nAChR chimeras by analyzing the amount of radioactivity present. The [^{3}H]epibatidine had a specific activity of 55.8Ci/mol and was added to microwells of oocyte lysate at a 1.0 nM concentration. The disintegrations per minute (DPM) were measured and used to calculate the bound [^{3}H]epibatidine per oocyte determining the receptor's function.

α7 M1 was used to create a homopentameric M1 in α4β2 subunits in an attempt to create a heteromer with a single M1 structure similar to the 5HT3A structure. The large number of residue similarities among the nAChR subunits and previous studies on α4α7M1 and β2α7M1 predicted that the chimera would retain the native binding ability. The ligand binding values seen above each histogram bar measure the yield of functional receptors (Fig. 6). The ligand binding assay determined that α4α7M1 and β2α7M1 had decreased [^{3}H]epibatidine binding compared to the native α4β2 M1 receptor. This was unexpected and consequently defines the few mutated residues of the α4β2 M1 as important for the high binding ability of α4β2 M1 receptors.

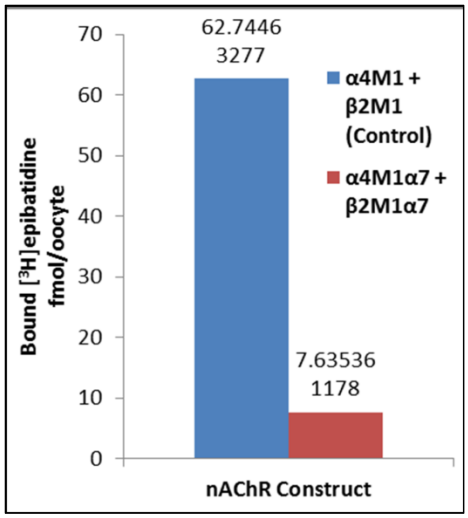

Figure 6. α4α7M1 and β2α7M1 had decreased [^{3}H]epibatidine binding compared to the native α4 and β2 M1 subunits with a decrease of approximately ten-fold of the ligand binding ability (fmol/oocytes).

After analyzing the variances between the 5HT3A M1 and α7 M1, the disparities of the amino acid characteristics were ranked from a predicted conservation of function to a predicted loss of function. Yellow mutations represented a hypothesized insignificant mutation with respect to binding ability. The mutation succession extended to green, blue, and finally red which was predicted to consist of deleterious mutations. It was hypothesized that as mutations with dissimilar properties compared to the native amino acids were added in binding ability would decrease. The [^{3}H]epibatidine binding assay confirmed this prediction as mutations with severely disparate characteristics compared to the native residue created a large decrease in function (Fig. 7). The yellow mutations, however, did not have as great of a negative effect on the receptor binding. The binding assay concluded that mutations with dissimilar characteristics compared to native residues create greater unfavorable effects on protein function than residues with similar properties.

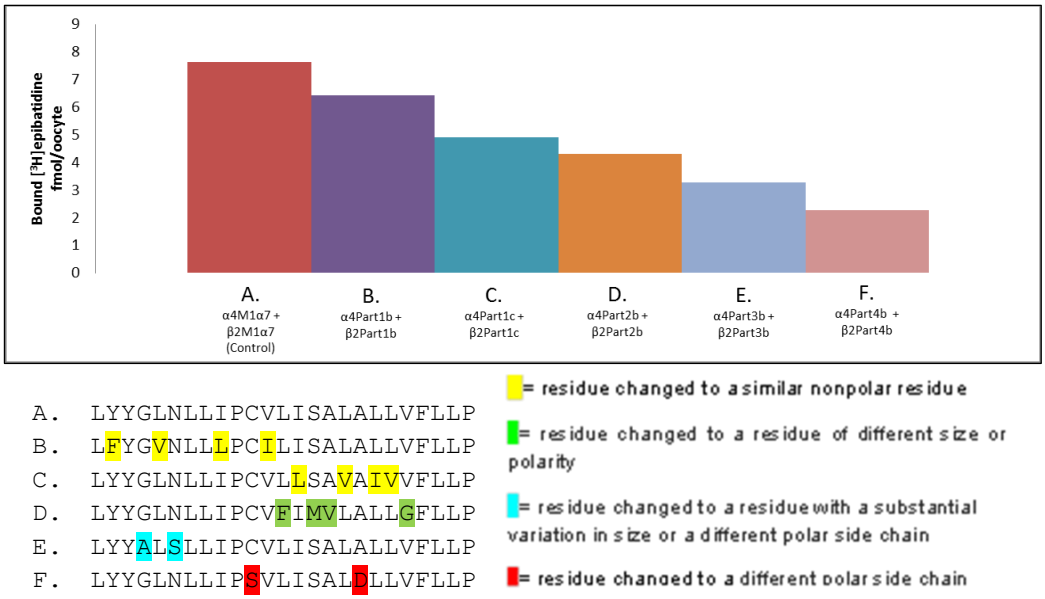

Figure 7. Compared to the control, α4α7M1 and β2α7M1, adding in 5HT3A residues with a progressive change from the native amino acid characteristic caused a gradual decrease in [^{3}H]epibatidine binding.

The collective progression of mutations from yellow to red was predicted to cause diminished [^{3}H]epibatidine binding due to the accumulation of altered residues. It was concluded that as the quantity of mutations increased, the ligand binding ability decreased compared to the control, α4α7M1 and β2α7M1 (Fig.8). The yellow mutations caused a larger decrease in binding ability than predicted. With the high conservation of native characteristics in the yellow mutations, we expected retention of the binding ability of the control. These unexpected results may be due to residue interactions in subunit assembly.

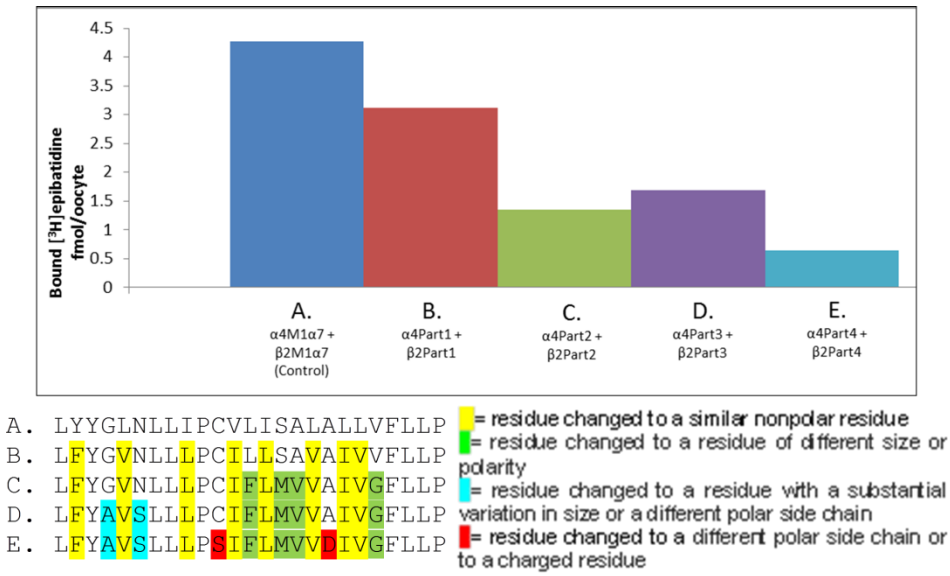

Figure 8. Compared to the control, α4α7M1 and β2α7M1, as the α7 to 5HT3A mutations were made a decrease in [^{3}H]epibatidine binding was observed.

A pentamer composed of five mutated subunits resulted in decreased binding abilities in all mutated constructs. However, it was predicted that constructing a receptor from both native and mutated subunits would result in higher binding abilities. The [^{3}H]epibatidine determined the combinatorial effect of native and mutated subunits to increase binding ability (Fig. 9). When one of the subunit types, α4 or β2, was composed of a native M1, the function of the receptor increased. Consequently, native subunits may aid in the proper folding and function of nAChR with chimeric subunits.

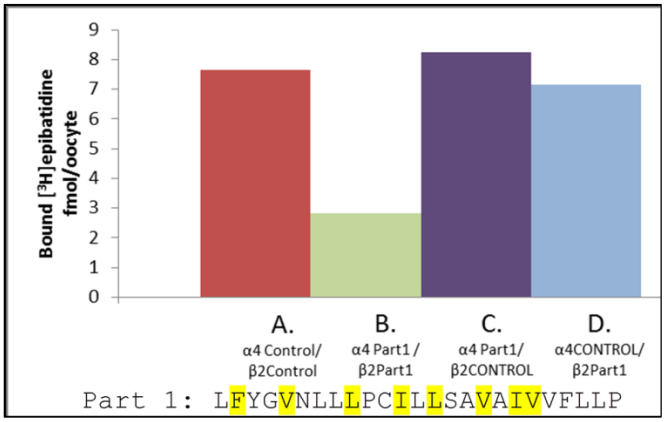

Figure 9. Heteromers composed of both mutated α4 β2 subunits had decreased binding compared to receptors with one native subunit type.

Immunoblotting

In order to induce protein expression, the truncated nAChRs with varying levels of mutagenesis were injected into the *Xenopus laevis* oocytes. The positive controls conducted alongside the mutated constructs were α4M1α7 and β2M1α7. The negative control contained only uninjected oocytes. Using a 12.5% acrylamide gel, the proteins were purified and separated. Immunoblotting was conducted with the mAb142 and mAb236 antibody to identify the α4 and β2 subunits, respectively (Fig. 10 and 11).

The control and mutant constructs were predicted to have equivalent amounts of total protein present. The immunoblots confirmed the presence of protein. However, the protein concentrations were not uniform throughout the mAb142 and mAb236 blots. The variation in protein may be due to differential protein degradation rates of the constructs. Further investigation will be needed to conclude the cause of the disparity in protein concentrations.

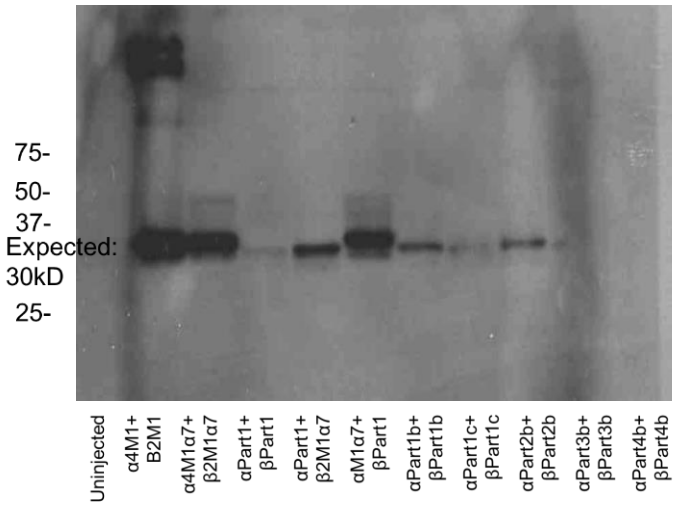

Figure 10. Immunoblot analysis displays a sufficient amount of protein present for each construct identified with the α4 mAb142 tag.

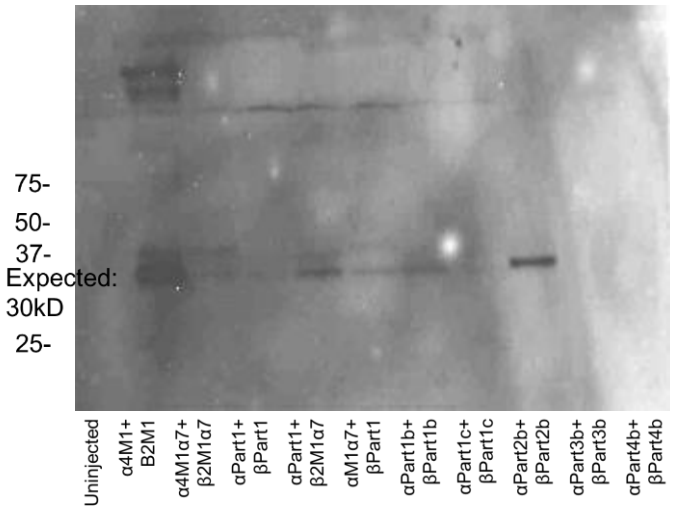

Figure 11. Immunoblot analysis displays a sufficient amount of protein present for each construct identified with the β2 mAb236 tag.

CHAPTER IV

CONCLUSIONS

Viability of a Homomeric M1 within Truncated α4β2 Subunits

5HT3A and α7 nAChR are both homomeric receptors. Understanding the assembly of homomeric receptors will contribute to our comprehension of the complex assembly of heteromeric receptors such as α4β2 receptors. In order to fully grasp the role of M1 in not only ECD function but subunit assembly, it is critical to determine if a homomeric M1 is viable in α4β2 receptors. While previous studies have shown that α4M1α7 and β2M1α7 retain function at a level comparable to the native α4M1 and β2M1 (Fig. 2), our results showed that this M1 substitution caused a large decrease in function (Fig. 6). It was assumed that α4M1α7 and β2M1α7 would be a reliable starting point with high expression based on the previous experimental results and high homology. Nevertheless, there was enough binding ability present to continue with the α7-5HT3A mutagenesis and study the effect of additional mutations on nAChR's M1. The unpredicted results have led to further questioning of what composes a feasible M1. Future studies will assess whether α4 M1 replacing the β2 M1 creates a viable receptor and reciprocally for the α4 receptor.

α4β2 Subunit Roles in Receptor Assembly

Our α4M1α7 and β2M1α7 results revealed that altering a native M1 to an exceedingly similar M1 will inhibit proper subunit assembly. This was unexpected as we had predicted the small number of mutations would have an insignificant effect on the ligand binding ability. We then sought to study the combinatorial effect of native and mutated subunits forming heteromeric

proteins (Fig. 9). When both α4M1 and β2M1 were mutated, there was a substantial decrease in ECD function. However, when one of the subunit types, α4 or β2, was composed of a native M1, the binding ability increased. This is significant because it shows a potential relationship in native subunits aiding the assembly of a functional receptor even in the presence of mutations. Additional structural and protein folding studies will have to be conducted, but native subunits may assist in the proper folding and function of chimeric nAChRs.

Effect of Mutations on ECD Function

The [^{3}H]epibatidine binding results concluded that mutations with severely disparate characteristics compared to the native residue created a large decrease in function. This was expected, as adding in a residue with a substantial variation in charge or size would undoubtingly affect the protein structure. However, the reduction of function seen with mutations to similar residues was unexpected. While the amino acid changes to analogous nonpolar residues were not predicted to affect the protein structure, our results led us to conclude that these appearingly insignificant mutations impacted the overall folding of the protein. In summary, the α7 amino acid conversions to 5HT3A were ranked from unfavorable effects (yellow) to deleterious effects (red) and these results were then visualized on the M1 structure (Fig. 12). This structure allows the layout of the ranging mutations and the possible protein interactions that could be affected by specific mutations to be conceptualized.

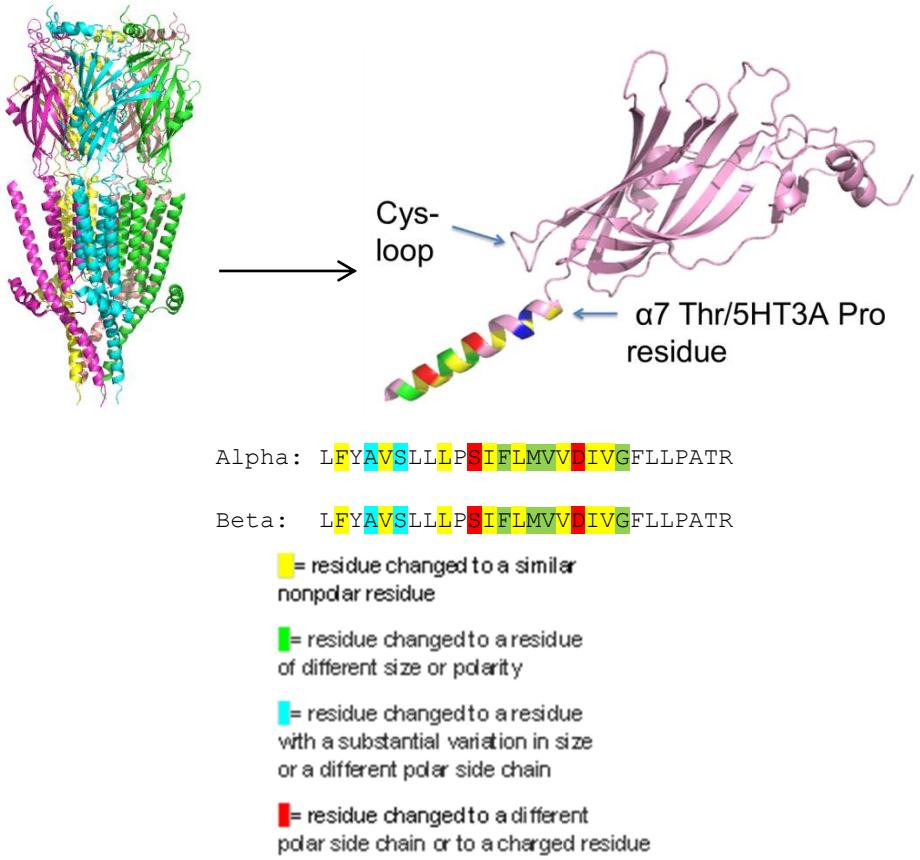

Figure 12. The [^{3}H]epibatidine binding results were used to determine the mutations most detrimental to ECD function. These conclusions were then applied to the three-dimensional structure of the M1 allowing residual interactions to be visualized.

A specific mutation of interest when considering residual interactions was the conversion of cysteine to serine in Part 4. This mutation is significant as a large quantity of Cys-loop receptors have this cysteine present alongside a proline. With the strong residual conservation throughout the receptor family, it was assumed that this mutation would have a negative effect on the feasibility of the M1. This was seen to be true and leads us to continue questioning what role this residue plays in transmembrane domain assembly as well as subunit assembly.

After analyzing the M1 amino acid composition, another residue of particular importance was distinguished. The proline at the front of the M1 structure is conserved in α4, β2, and 5HT3A

(Fig. 13). Notably, there is a threonine present at this location in the α7 M1. This discrepancy allows us to ponder whether reverting this residue back to the α4β2 native proline would create a higher functioning α4M1α7 and β2M1α7 construct.

```
LGICdbp: 5HT3Amumu-1          -ISNSYAEMKFYVIIRRRPLFYAVSLLLPSIFLMVVDIVGFCLPPDSGERVSFKITLLLG
LGICdbp: ACHa7gaga            CCKEPYPDITFTVTMRRRTLYYGLNLLIPCVLISALALLVFLLPADSGEKISLGITVLLS
LGICdbp: ACHa4hosa            CCAEIYPDITYAFVIRRLPLFYTINLIIPCLLISCLTVLVFYLPSECGEKITLCISVLLS
LGICdbp: ACHb2hosa            -DDSTYVDITYDFIIRRKPLFYTINLIIPCVLITSLAILVFYLPSDCGEKMTLCISVLLA
                                 . * ::.: . :**  *:* :.*::*.:::  : :: * ** :.**:::: *::**.

* = conserved amino acid   : = conservation of amino acid properties   . = semi-conservation of amino acid properties
```

Figure 13. The sequence alignment of 5HT3A, α7, α4, and β2 highlighting the dissimilarity of the α7 proline and 5HT3A, α4, and β2 threonine.

Not only do the α7 to 5HT3A mutations guide our insight into nAChR ECD function but additionally 5HT3A ECD function. While truncated ECD α4β2 receptors have been produced, a 5HT3A ECD structure has yet to be constructed. Our results will aid in future compositions of truncated 5HT3A structures allowing high resolution crystallized structures to be created.

The results of our [^{3}H]epibatidine binding assay allowed us to distinguish which amino acids were potentially important in the nAChR M1 and which 5HT3A residues could be considered detrimental to a nAChR M1. This data will advance structural studies attempting to understand the full-length nAChR and Cys-loop receptor superfamily as a whole. With the progression of our comprehension of receptor assembly, binding, and function, we aspire to develop novel truncated proteins retaining the characteristics of the full-length receptors. Resultantly, we seek to crystallize these structures aiding the development of possible drug design targeting the many diseases affected by the Cys-loop receptors.

REFERENCES

1. Nys, M., Kesters, D., and Ulens, C. (2013) Structural insights into Cys-loop receptor function and ligand recognition, *Biochemical Pharmacology 86*, 1042-1053.
2. Wells, G. B. (2008) Structural answers and persistent questions about how nicotinic receptors work, *Frontiers in bioscience : a journal and virtual library 13*, 5479-5510.
3. Lemoine, D., Jiang, R., Taly, A., Chataigneau, T., Specht, A., and Grutter, T. (2012) Ligand-gated ion channels: new insights into neurological disorders and ligand recognition, *Chemical reviews 112*, 6285-6318.
4. Brejc, K., van Dijk, W. J., Klaassen, R. V., Schuurmans, M., van Der Oost, J., Smit, A. B., and Sixma, T. K. (2001) Crystal structure of an ACh-binding protein reveals the ligand-binding domain of nicotinic receptors, *Nature 411*, 269-276.
5. Hilf, R. J., and Dutzler, R. (2008) X-ray structure of a prokaryotic pentameric ligand-gated ion channel, *Nature 452*, 375-379.
6. Bocquet, N., Nury, H., Baaden, M., Le Poupon, C., Changeux, J. P., Delarue, M., and Corringer, P. J. (2009) X-ray structure of a pentameric ligand-gated ion channel in an apparently open conformation, *Nature 457*, 111-114.
7. Unwin, N. (2005) Refined structure of the nicotinic acetylcholine receptor at 4A resolution, *Journal of molecular biology 346*, 967-989.
8. Dellisanti, C. D., Yao, Y., Stroud, J. C., Wang, Z. Z., and Chen, L. (2007) Crystal structure of the extracellular domain of nAChR alpha1 bound to alpha-bungarotoxin at 1.94 A resolution, *Nature neuroscience 10*, 953-962.
9. Stergiou, C., Zisimopoulou, P., and Tzartos, S. J. (2011) Expression of water-soluble, ligand-binding concatameric extracellular domains of the human neuronal nicotinic receptor alpha4 and beta2 subunits in the yeast Pichia pastoris: glycosylation is not required for ligand binding, *J Biol Chem 286*, 8884-8892.
10. Zouridakis, M., Zisimopoulou, P., Eliopoulos, E., Poulas, K., and Tzartos, S. J. (2009) Design and expression of human α7 nicotinic acetylcholine receptor extracellular domain mutants with enhanced solubility and ligand-binding properties, *Biochimica et Biophysica Acta (BBA) - Proteins and Proteomics 1794*, 355-366.
11. Lazaridis, K., Zisimopoulou, P., Giastas, P., Bitzopoulou, K., Evangelakou, P., Sideri, A., and Tzartos, S. J. (2014) Expression of human AChR extracellular domain mutants with improved characteristics, *International journal of biological macromolecules 63*, 210-217.
12. Kouvatsos, N., Niarchos, A., Zisimopoulou, P., Eliopoulos, E., Poulas, K., and Tzartos, S. (2014) Purification and functional characterization of a truncated human alpha4beta2 nicotinic acetylcholine receptor, *International journal of biological macromolecules 70*, 320-326.
13. Carpenter, E. P., Beis, K., Cameron, A. D., and Iwata, S. (2008) Overcoming the challenges of membrane protein crystallography, *Current opinion in structural biology 18*, 581-586.
14. McKinnon, N. K., Bali, M., and Akabas, M. H. (2012) Length and amino acid sequence of peptides substituted for the 5-HT3A receptor M3M4 loop may affect channel expression and desensitization, *PloS one 7*, e35563.

15. Hassaine, G., Deluz, C., Grasso, L., Wyss, R., Tol, M. B., Hovius, R., Graff, A., Stahlberg, H., Tomizaki, T., Desmyter, A., Moreau, C., Li, X. D., Poitevin, F., Vogel, H., and Nury, H. (2014) X-ray structure of the mouse serotonin 5-HT3 receptor, *Nature 512*, 276-281.
16. Sobolevsky, A. I., Rosconi, M. P., and Gouaux, E. (2009) X-ray structure, symmetry and mechanism of an AMPA-subtype glutamate receptor, *Nature 462*, 745-756.
17. Miller, P. S., and Aricescu, A. R. (2014) Crystal structure of a human GABAA receptor, *Nature 512*, 270-275.
18. Hibbs, R. E., and Gouaux, E. (2011) Principles of activation and permeation in an anion-selective Cys-loop receptor, *Nature 474*, 54-60.
19. Pons, S., Sallette, J., Bourgeois, J. P., Taly, A., Changeux, J. P., and Devillers-Thiery, A. (2004) Critical role of the C-terminal segment in the maturation and export to the cell surface of the homopentameric alpha 7-5HT3A receptor, *The European journal of neuroscience 20*, 2022-2030.
20. Anand, R., Conroy, W. G., Schoepfer, R., Whiting, P., and Lindstrom, J. (1991) Neuronal nicotinic acetylcholine receptors expressed in Xenopus oocytes have a pentameric quaternary structure, *J Biol Chem 266*, 11192-11198.
21. Brody, A. L., Mukhin, A. G., La Charite, J., Ta, K., Farahi, J., Sugar, C. A., Mamoun, M. S., Vellios, E., Archie, M., Kozman, M., Phuong, J., Arlorio, F., and Mandelkern, M. A. (2013) Up-regulation of nicotinic acetylcholine receptors in menthol cigarette smokers, *The international journal of neuropsychopharmacology / official scientific journal of the Collegium Internationale Neuropsychopharmacologicum 16*, 957-966.
22. Albuquerque, E. X., Pereira, E. F., Alkondon, M., and Rogers, S. W. (2009) Mammalian nicotinic acetylcholine receptors: from structure to function, *Physiological reviews 89*, 73-120.
23. Wells, G. B., and Person, A. (2005) Role of the First Transmembrane Domain in Expression of α4β2 Nicotinic Acetylcholine Receptors, *35th Annual Meeting of the Society for Neuroscience (Neuroscience 2005)*.
24. Wang, Z. Z., Hardy, S. F., and Hall, Z. W. (1996) Assembly of the nicotinic acetylcholine receptor. The first transmembrane domains of truncated alpha and delta subunits are required for heterodimer formation in vivo, *J Biol Chem 271*, 27575-27584.
25. Wells, G., and Person, A. (2008) Specific residues of first transmembrane domains affect expression of extracellular domain (alpha4)(beta2) nicotinic acetylcholine receptors, In *38th Annual Meeting of the Society for Neuroscience (Neuroscience 2008)*.